Colloid Polym Sci 273:1144–1150 (1995)

ORIGINAL CONTRIBUTION

K. Gotoh
A. Yasukawa
M. Ohkita
H. Obata
M. Tagawa

Wettability and surface free energy of electrolytically oxidized graphite fibers

Received: 17 May 1995
Accepted: 13 July 1995

K. Gotoh
Faculty of Education
Kyoto University of Education
1 Fukakusa-Fujinomori-cho, Fushimi-ku
Kyoto 612, Japan

A. Yasukawa
School of Chemistry
Osaka University of Education
4-698-1 Asahigaoka, Kashihara-shi
Osaka 582, Japan

M. Ohkita · H. Obata
Prof. Dr. M. Tagawa (✉)
Department of Textile & Apparel Science
Nara Women's University
Kita-uoya-higashi-machi, Nara-shi
Nara 630, Japan

Abstract Wettability of electrolytically oxidized graphite fibers has been investigated by contact angle measurements employing the Wilhelmy method. The atomic ratio of oxygen to carbon, O/C, in the surface layer of the graphite fiber increased with increasing electric specific charge. Contact angle hysteresis was not observed for the untreated graphite fiber (O/C = 0.01). The contact angles decreased with increasing O/C, especially for the receding angle, and approached constant for O/C > 0.2. The nondispersive and dispersive surface free energies of the oxidized graphite fibers were calculated from the experimentally determined contact angles. The nondispersive surface free energy increased by the oxidation, whereas the dispersive one decreased. From the results of surface analysis, it was found that the changes in the nondispersive and dispersive surface free energies were caused by the increase in O/C ratio and the decrease in surface crystallinity, respectively.

Key words Wettability-surface free energy – contact angle – carbon fiber – graphite fiber

Introduction

In recent years many investigations of wetting of solid surfaces have been carried out because of the fundamental interest as well as the practical importance. Wettability has been most commonly described by the contact angle and the surface free energy. The theoretical calculation of the surface free energy is difficult because of its sensitivity to atomic or chemical composition and molecular orientation at the surface [1, 2]. For rigid, smooth and homogeneous surfaces, contact angles can be related to surface free energies by the well-known Young's equation from a force balance at the three-phase boundary. Hence, the surface free energy can be experimentally estimated by the contact angle measurements.

In most cases, experimentally observed contact anlges for real surfaces have hysteresis [3, 4], which causes the difficulty in the experimental determination of the surface free energy. Therefore, the experimental determination of "thermodynamically significant contact angles" [5] is necessary for real surfaces having contact angles hysteresis. The obtained equilibrium contact angles are useful for better understanding of wetting behavior of the real surfaces.

In this paper, we present an experimental study on wetting of real surfaces using graphite fibers which are manufactured from polyacrylonitrile (PAN) fibers by carbonization and graphitization techniques. The main structural elements of the PAN based graphite fibers are graphite ribbons that lie parallel to the fiber axis [6]. This structure gives homogeneity and low energy to the surface because the surface is mostly composed of graphite basal planes.

Graphite fibers are used as the reinforcing agent in structural polymeric matrix composite materials. The molecular interaction between the polymeric matrix and the reinforcing fiber at fiber matrix interface is important for composite mechanical performance and durability [7, 8]. Since the graphite fibers are inactive, the surface treatment of the fibers is frequently done to improve adhesion between the matrix and the fibers [9–14]. Electrolytic oxidation is one of the commercial surface treatments [15–17], which proivides additional functional groups to the fiber surface. Although the surface free energy of the oxidized graphite fiber has been experimentally determined by Tsutsumi et al. [18], the effect of oxidation has not been investigated in detail by using graphite fibers with different degree of oxidation.

The experimental estimation of the surface free energy of the oxidized graphite fiber is not only important from the practical point of view, but also give fundamental information about the wettability of heterogeneous surfaces or real surfaces because the surface of the oxidized graphite fiber can be considered to be the predominantly low-energy surface with fractional high-energy regions.

This study is dealing with the changes in the surface free energy and in surface chemical composition with the electrolytic oxidation of the PAN based graphite fibers. We have measured contact angles in the graphite fiber/n-alkane/water systems by the wetting force measurements employing the Wilhelmy technique. The dispersive and nondispersive components of the surface free energies were calculated from the angles obtained with a series of n-alkanes. The results were discussed in terms of chemical composition and crystallinity of the fiber surface.

Experimental

Materials

Polyacrylonitrile (PAN) based graphite fibers studied here were the high tension (HT) and high modulus (HM) types. They were prepared on a laboratory scale in Toray Industries Inc., and no additional surface sizing was done. The strength and modulus of the fibers are given in Table 1.

Table 1 Untreated polyacrylonitrile based graphite fibers

Fibers	Strength (kgf/mm^2)	Modulus (10^2 kgf/mn^2)
HT	350	245
HM	290	403

The electrolytic oxidation of the graphite fibers was performed in an aqueous sulfuric acid solution [15, 17]. The surfaces of the untreated and oxidized fibers were analyzed by means of x-ray photoelectron spectroscopy (XPS) using an AEI-Kokusai Denki model ES-200 with an $\mathrm{AlK}_{\alpha_{1,2}}$ x-ray anode ($h\nu = 1486.6$ eV). The base pressure was 10^{-8} Torr. Samples were prepared by cutting a number of fibers and placing them into a sample holder. The details of the XPS measurements have been described in the literature [17]. The fiber surfaces were observed by the scanning electron microscope.

The graphite fibers were successively purified by extraction with water, ethanol, and ethyl ether prior to use. Extrapure grade n-alkanes (n-pentane, n-hexane, n-heptane, n-octane, n-nonane and n-decane) and doubly distilled water were used for the contact angle measurements.

Contact angle measurements

Advancing and receding contact angles of water in the graphite fiber/n-alkane/water systems were measured by the Wilhelmy method using an electrobalance (Cahn Instruments Inc., C-2000) and a reversible elevator (Burleigh Instruments Inc., Inchworm Motor). The experimental details have been reported elsewhere [19–22]. Weight recordings were obtained during a fiber immersion-emersion cycle at the velocity of 0.3 mm/min in the plateau region where the contact angles were independent of the velocity, since the contact angles in the plateau region are considered to be the "thermodynamically significant contact angles" [5, 20, 22]. The cycle was repeated twice or more for the same part on the same sample and reproducibility was checked.

A typical weight recording is illustrated in Fig. 1. The points a and c in the figure show the moments when the lower edge of the fiber touched the n-alkane/water interface and separated from the interface, respectively. At the point b, the interface is reversed in direction. The weight recording during advancing and receding scans had no slope due to buoyancy. The mean advancing and receding contact angles of water were calculated by the Wilhelmy equation from the weight changes at the points a and c (i.e., ΔW_a and ΔW_r), respectively. For the calculation of contact angles, the effective perimeter of each fiber was determined from the weight recording obtained at the n-pentane/air interface since the contact angle in this system can be regarded as zero [20].

Contact angle measurements were carried out in a room maintained at a constant temperature (20 °C) and a constant relative humidity (65%).

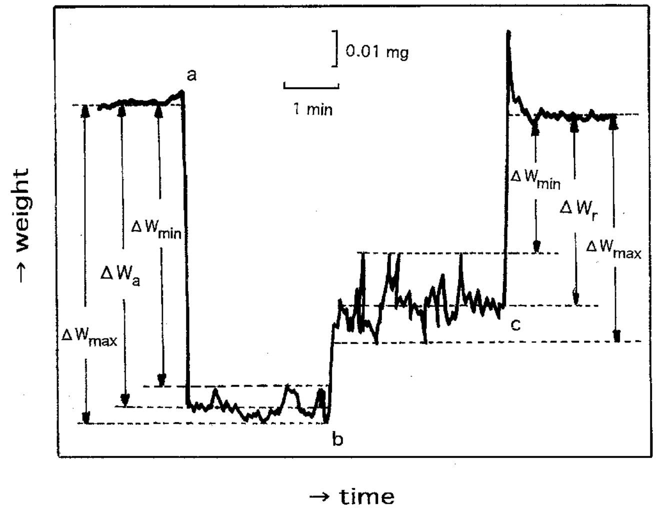

Fig. 1 A typical weight recording for an untreated HT graphite fiber/water/*n*-octane system

Results and discussion

Surface analysis of the fibers

The atomic ratio of oxygen to carbon, O/C, in the surface layer calculated from the XPS data is shown in Fig. 2 as a function of specific electric charge. In either case of the HT and HM graphite fibers, the O/C ratio increased with increasing specific electric charge. The scanning electron micrographs of the graphite fibers are shown in Figs. 3 and 4. The fibers have diameters of ca. 6 μm and grooves parallel to the fiber axis. The morphological changes in the fiber surfaces due to oxidation were not observed for both HT and HM fibers.

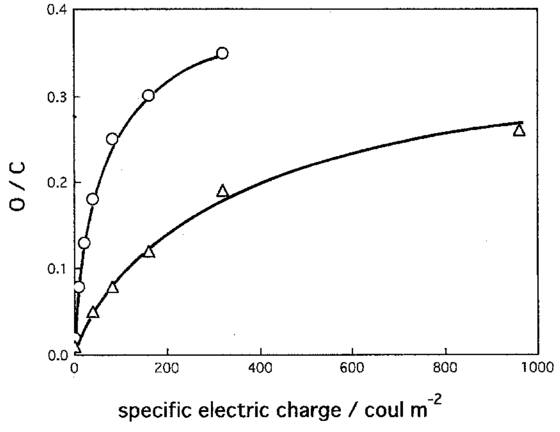

Fig. 2 The carbon/oxygen atomic concentration ratio at oxidized HT (○) and HM (△) graphite fiber surfaces, O/C, as a function of specific electric charge

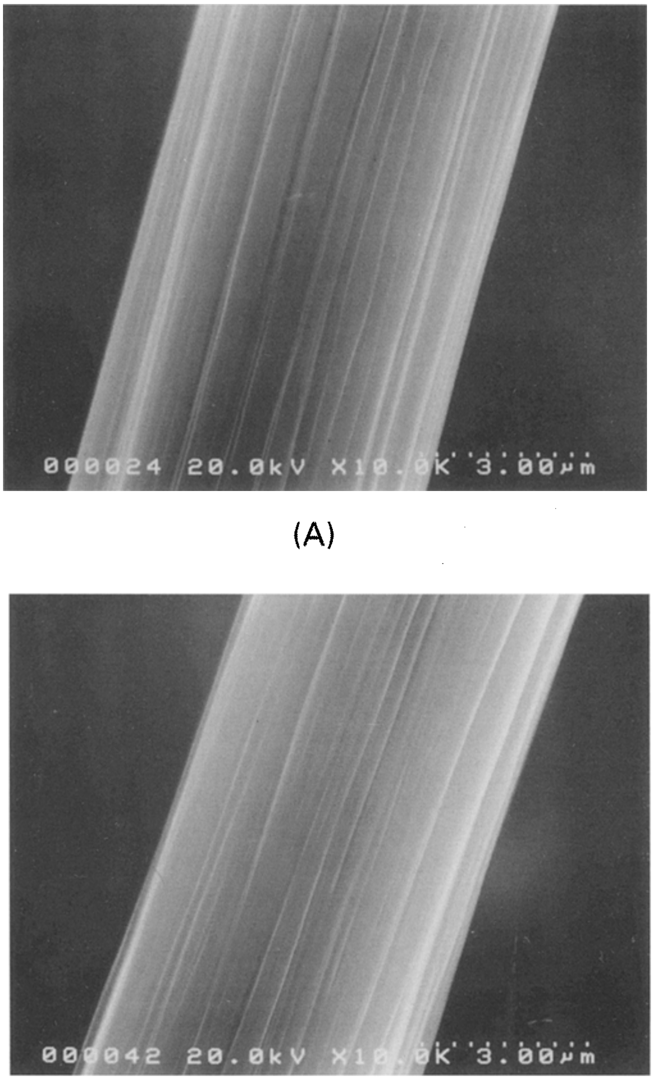

(A)

(B)

Fig. 3 Scanning electron micrographs of untreated (A) and oxidized (B, 320 coul m^{-2}) HT graphite fibers

Effect of surface oxygen concentration on contact angles

Contact angles of water, θ, obtained in the graphite fiber/*n*-hexane/water systems are given in Fig. 5 as a function of the atomic ratio of oxygen to carbon in the surface layer, O/C. The advancing and receding angles decreased with increasing O/C ratio, and they became almost constant for O/C > 0.2. For O/C < 0.1, the receding angle was sensitive to the small change in the O/C ratio compared with the advancing one. The results of the HT and HM fibers were plotted on the same line. The same trend as the curves for the *n*-hexane/water system in Fig. 5 was observed when the other *n*-alkanes were used.

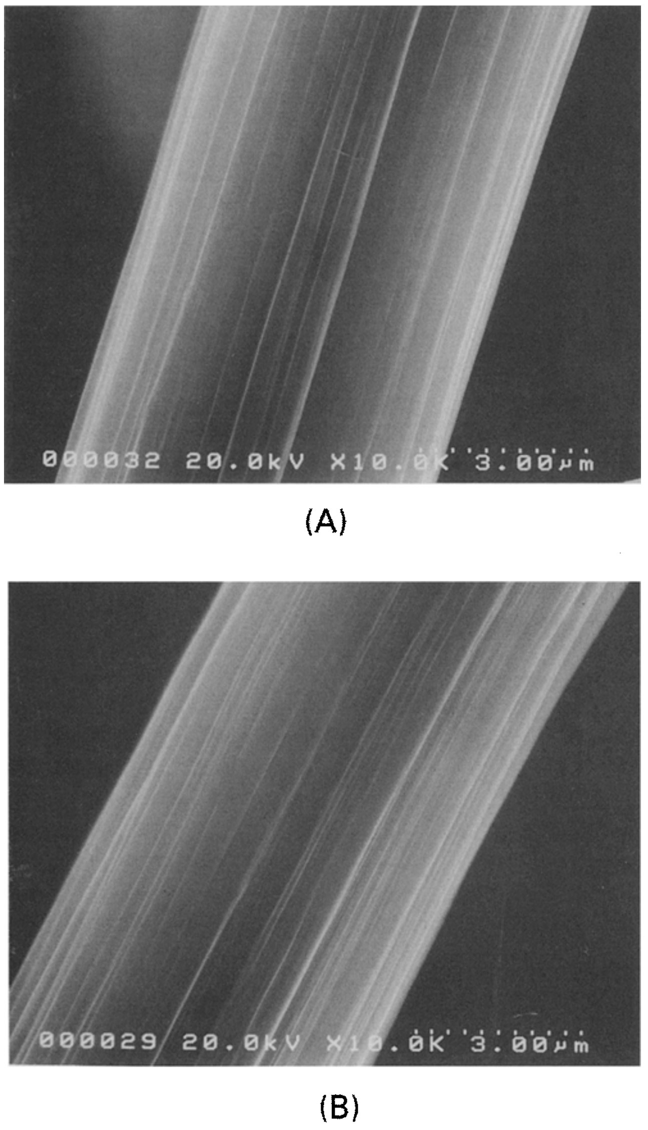

Fig. 4 Scanning electron micrographs of untreated (A) and oxidized (B, 640 coul m^{-2}) HM graphite fibers

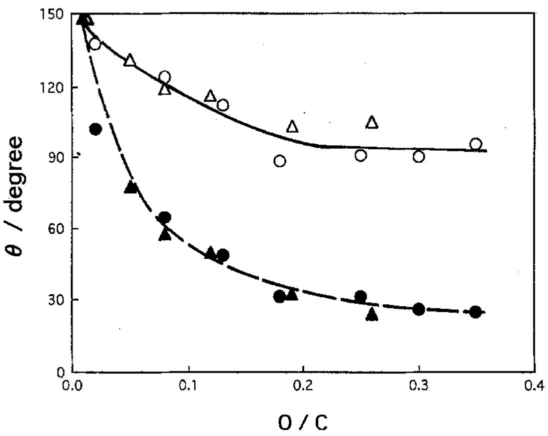

Fig. 5 Relation between advancing (○, △) and receding (●, ▲) contact angles of water and the carbon/oxygen atomic concentration ratio, O/C, at the fiber surface, in HT (○, ●) or HM (△, ▲) graphite fiber/water/*n*-hexane systems

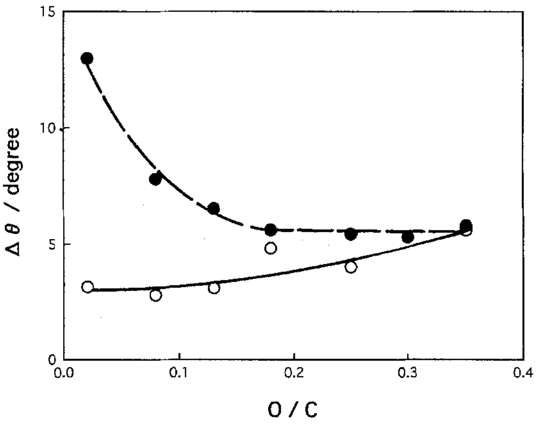

Fig. 6 Relation between the local deviation in advancing (○) and receding (●) contact angles of water and the carbon/oxygen atomic concentration ratio at the fiber surface, O/C, in HT graphite fiber/water/*n*-hexane systems

In Fig. 1, the local deviation in weight trace is shown during advancing and receding scans. The local deviation was reproducibly observed for all systems in the present study. In the previous paper [22], we have reported the similar deviation in various fibers/*n*-alkane/water systems, and have concluded that the contact angle calculated from ΔW_a or ΔW_r corresponds to the mean angle and that the deviation in weight trace includes a local deviation in the contact angle due to heterogeneity as well as a deviation in perimeter of the fiber along the three-phase boundary during immersion and emersion. In this study, the maximum and minimum contact angles on the same fiber surface were calculated from ΔW_{max} and ΔW_{min} in Fig. 1, respectively, by considering maximum and minimum perimeters of the fiber which were estimated from the weight trace at the *n*-pentane/air interface in the same manner [22]. The maximum and minimum perimeters obtained from the weight trace were 23.3 µm and 22.5 µm for the untreated HT fiber, respectively. The difference between the maximum and minimum angles was expressed by $\Delta\theta$ as the local deviation in contact angle.

Figure 6 shows the local deviation in contact angle, $\Delta\theta$, at the *n*-hexane/water interface as a function of the O/C ratio. The values of $\Delta\theta$ are large in receding, especially at the small value of the O/C ratio. Considering that the local deviation in contact angle is caused by the change in atomic concentration of oxygen from point to point on the heterogeneous graphite fiber surface, it is expected that $\Delta\theta$ is large when the dependence of the contact angle on the O/C ratio is large. The experimental facts are consistent with this expectation; the O/C dependence of θ is large in receding for O/C < 0.1 (Fig. 5), and the $\Delta\theta$ values are also large under the same condition (Fig. 6).

As can be seen in Fig. 5, contact angle hysteresis was observed for all graphite fibers except the untreated HM fiber (O/C = 0.01). Contact angle hysteresis increased with increasing O/C ratio. In general, contact angle hysteresis can be caused by surface roughness, surface heterogeneity, penetration of a wetting liquid, deformation, reorientation and surface mobility during the contact angle measurements. In the present study, the penetration is not a serious cause of hysteresis because of the reproducibility of the weight recording for the same sample. The differences in surface topography between the untreated HT and untreated HM graphite fibers were not found, and no morphological changes on the fiber surface were produced by the oxidation (see Figs. 3 and 4). In addition, deformation, reorientation and surface mobility is not expected because the fiber surface is composed of graphite basal plane. Therefore, we concluded that the contact angle hysteresis here was caused by surface heterogeneity. In our previous studies [19, 21], the contact angle hysteresis was observed in commercially available HM PAN-based carbon fibers pyrolyzed at 2500 °C, and disappeared after repyrolyzation at 3000 °C in vacuum [19]. When atomic oxygen irradiation was applied to the repyrolyzed carbon fibers, the hysteresis was again observed [21]. Scanning electron micrographs and Auger electron spectroscopic analysis showed that surface heterogeneity is a dominant factor causing the contact angle hysteresis; no hysteresis appeared for the repyrolzed carbon fiber whose surface has 1% oxygen other than carbon atoms and the hysteresis became larger with respect to atomic concentration of oxygen at the fiber surfaces. These results in the previous studies are in accordance with the results in Fig. 5.

Johnson and Dettre [23] have calculated the contact angle of a liquid drop on a model heterogeneous surface having regions of different intrinsic wettabilities. According to their calculation, in the case of the predominantly low-energy surface with fractional high-energy regions, the receding contact angle varied with the precentage of the high-energy region whereas the advancing one remained almost constant or slightly decreased. Considering that surface oxygen concentration corresponds to the percentage of the high-energy region, the plots of the receding contact angles against surface oxygen concentration for the oxidized graphite fibers (Fig. 5, closed symbols) have the same tendency as their calculated curve.

However, the decrease in the advancing angles with surface oxygen concentration (Fig. 5, open symbols) is noticeable compared with the calculated curve [23]. In the case of the carbon fibers exposed to atomic oxygen mentioned above, the advancing angle was constant with increasing surface oxygen concentration [22]. Dettre and Johnson [24] have experimentally found that the wettability of a heterogeneous surface relates to the intrinsic wettabilities of high-energy or low energy regions as well as the sizes and shapes of the regions; the advancing contact angle decreases with increasing percentage of high-energy regions when the intrinsic wettabilities of the regions change with keeping their sizes and shapes constant, whereas the advancing angle is independent of the percentage of high-energy regions when the sizes and shapes of the regions change without changing their intrinsic wettabilities. On the basis of their findings and our results, we assume that the oxidation by the electrolysis gives the qualitative change (i.e., the change in the intrinsic wettability) in the high-energy regions on the fiber surface whereas the oxidation by the atomic oxygen exposure gives the quantitative change (i.e., the change in the sizes and shapes). A more detail investigation is needed to verify our assumption.

Estimation of surface free energies

Assuming that the Young's equation holds in the graphite fiber/n-alkane/water system, one can obtain the expression using the extended Fowkes' equation with respect to the surface free energy [19–21]

$$\gamma_w - \gamma_o + \gamma_{ow}\cos\theta = 2(\gamma_s^d)^{1/2}[(\gamma_w^d)^{1/2} - (\gamma_o)^{1/2}] + 2(\gamma_s^{nd}\gamma_w^{nd})^{1/2} \qquad (1)$$

where γ is the surface free energy, θ is the contact angle of water, the subscripts *s*, *w*, and *o* refer to solid, water, and n-alkane, and the superscript *d* and *nd* refer to dispersive and nondispersive components, respectively. The relations between $\gamma_w - \gamma_o + \gamma_{ow}\cos\theta$ and $(\gamma_w^d)^{1/2} - (\gamma_o)^{1/2}$ which were obtained by using the experimentally determined contact angles showed straight lines. The linear relations indicate that the three phase boundary of graphite fiber/n-alkane/water is formed, i.e., that the adsorption layer of n-alkane on the fiber does not give a serious effect on the contact angles. The dispersive and nondispersive surface free energies were calculated from the slope and the intercept of the plot. The dispersive and nondispersive components of the surface free energy were determined from the advancing and receding contact angles, respectively [20, 21].

The relation between the nondispersive surface free energy, γ_s^{nd}, and O/C is shown in Fig. 7. The γ_s^{nd} values

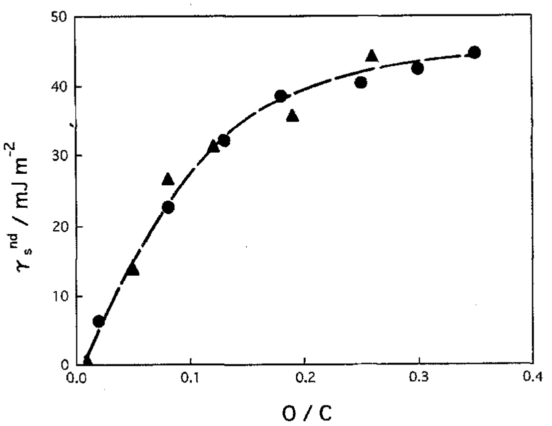

Fig. 7 Relation between nondispersive surface free energies of HT (●) and HM (▲) graphite fibers and the carbon/oxygen atomic concentration ratio at the fiber surface, O/C

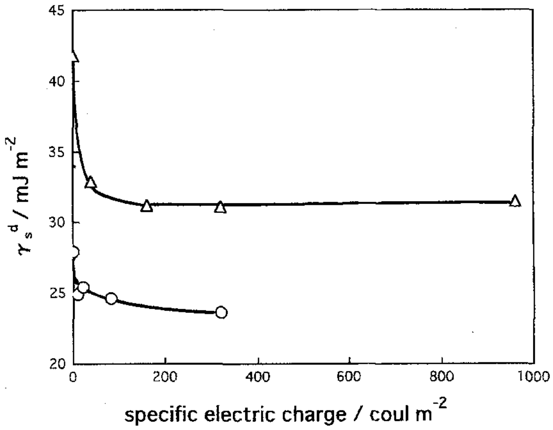

Fig. 8 Relation between dispersive surface free energies of HT (○) and HM (△) graphite fibers and the carbon/oxygen atomic concentration ratio at the fiber surface, O/C

increased with increasing O/C, and approached a constant value above O/C = 0.2.

In Fig. 8 the dispersive surface free energy, γ_s^d, is plotted as a function of specific electric charge. The γ_s^d value of the untreated HM fiber was larger than that of the untreated HT fiber. The degree of the axial preferred orientation of the fiber was determined to be 0.81 and 0.90 for the untreated HT and untreated HM fibers, respectively, by x-ray diffractiometry. Considering that the high degree of orientation in bulk is corresponding to the high degree of orientation at the surface, one can expect that the γ_s^d value associated with the surface concentration of interacting volume elements [25] is larger for the HM fibers compared with the HT ones. The results in Fig. 8 are consistent with this expectation. In either case of the HT and HM fibers, γ_s^d decreased by the electrolytic oxidation. The degrees of noncrystallinity of untreated and oxidized (160 coul m^{-2}) HM fibers were determined to be 0.36 and 0.76, respectively, from the ratio of peak intensity of 1355 cm^{-1} to 1580 cm^{-1} in Raman spectra. This suggets that the decrement of surface crystallinity by oxidation caused the decrease in dispersive surface free energies.

Conclusion

The advancing and receding contact angles of water were measured by the Wilhelmy method using the electrolytically oxidized graphite fibers with different atomic ratio of oxygen to carbon, O/C, in the surface layer. The advancing and receding angles decreased with increasing O/C ratio, and they approached constant above O/C = 0.2. The receding angle was sensitive to small changes in the O/C ratio for O/C < 0.1. Contact angle hysteresis was not detected for untreated high modulus graphite fiber (O/C = 0.01), and increased with increasing O/C ratio by the oxidation. The relation between the contact angle and the O/C ratio was explained by considering the oxidized graphite fiber surface to be a heterogeneous surface having regions of different intrinsic wettabilities.

The nondispersive and dispersive surface free energies of the oxidized graphite fibers were determined from the contact angles. The nondispersive surface free energy increased with increasing O/C ratio. The dispersive surface free energy decreased with increasing electric specific charge, which was caused by the decrease in surface crystallinity due to oxidation.

Acknowledgement The authors wish to express their gratitude to Toray Industries Inc. for offering the graphite fibers and for their surface analysis.

References

1. Sacher E (1983) J Colloid Interface Sci 92:275
2. Tagawa M, Gotoh K, Yokokura M, Syutoh A, Takechi S (1989) Colloid Polym Sci 267:434
3. Morra M, Occhiello E, Garbassi F (1990) Advan Colloid Interface Sci: 32:79
4. Johnson RE, Jr, Dettre RH (1969) In: Surface and Colloid Science Vol. 2. John Wiley & Sons, p 93
5. Cain JB, Francis DW, Venter RD, Neumann AW (1983) J Colloid Interface Sci 94:123
6. Diefendorf RJ, Takarsky E (1975) Polymer Engineering and Science 15:150

7. Dwight DW, Fowkes FM, Cole DA, Kulp MJ, Sabat PJ, Salvati L, Jr, Huang TC (1990) J Adhesion Sci Technol 4:619
8. Hsieh YL, Wu M, Andres D (1991) J Colloid Interface Sci 144:127
9. Donnet JB, Brendle M, Dhami TL, Bahl OP (1986) Carbon 24:757
10. Donnet JB, Dhami TL, Dong S, Brendle M (1987) J Phys D: Appl Phys 20:269
11. Hammer GE, Drzal LT (1980) Applications of Surface Science 4:340
12. Drzal LT, Mescher JA, Hall DL (1979) Carbon 17:375
13. Takahagi T, Ishitani A (1984) Carbon 22:43
14. Chabert B, Hoffmann P, Sage D, Soulier JP (1988) J Colloid Interface Sci 124:375
15. Shindo A (1988) Proc Intern Conf Interfaces in Composite Materials, S. P. E. Benelux Lieg
16. Fitzer E, Jager H, Popovska N, Sturm FV (1988) J Appl Electrochem 18:178
17. Nakayama Y, Soeda F, Ishitani A (1990) Carbon 28:21
18. Tsutsumi K, Ishida S, Shibata K (1990) Colloid Polym Sci 268:31
19. Tagawa M, Ohmae N, Umeno M, Gotoh K, Yasukawa A, Tagawa M (1989) Colloid Polym Sci 267:702
20. Tagawa M, Gotoh K, Yasukawa A, Ikuta M (1990) Colloid Polym Sci 268:589
21. Tagawa M, Ohmae N, Umeno M, Yasukawa A, Gotoh K, Tagawa M (1991) Japanese J Applied Physics 30:2134
22. Tagawa M, Yasukawa A, Gotoh K, Tagawa M, Ohmae N, Umeno M (1992) J Adhesion Sci Technol 6:763
23. Johnson RE, Jr, Dettre RH (1964) J Physical Chem 68:1744
24. Dettre RH, Johnson RE, Jr (1965) J Physical Chem 69:1507
25. Fowkes FM (1968) J Colloid Interface Sci 28:493